A study SARs for smart-watch model with monopole antenna

Seon-Eui Hong*, Jong-Hwa Kwon, and Hyung-Do Choi
EM Environment & Monitoring Research Group, Electronics and Telecommunication Research Institute, Daejeon, Korea

Abstract

Currently, the standard and regulations for specific absorption rate (SAR) testing of limb-worn devices specify the use of the flat phantom and the user's wrist is not considered. In this paper, the SARs for standard flat phantoms are calculated and compared with body shape phantom and anatomical human-body model. And we investigate the effect of wrist model during the SAR evaluation.

1. Introduction

Recently, the limb-worn devices market is outrageously growing. The international stands and regulations specify the methods to assess the SARs of smart-watch [1], [2]. In current version of international standard and regulation, the flat phantom is used a standard model and the user's wrist is not included for obtaining conservative SAR estimations. This raises the import query of whether the flat phantom provides sufficiently conservative estimation without considering the effect of the user's wrist. It is a great challenge to study the effect of the wrist in terms of SAR, since limb-worn devices and the wrist have complicated geometrics and are in the reactive near-antenna of limb-worn device. This paper will presents numerical computation results that quantify the effect of wrist model on SARs with the flat phantom, body shape model, and anatomical human-body model. We consider the SAR of electromagnetic (EM) radiation from smart-watch model with monopole antenna for operation at 835, 1850 MHz, and 2450 MHz.

2. Material and methods

2.1 Smart-watch model

The monopole antenna structures are widely used in wearable device [3]-[5]. In this study, the monopole antenna suitable for limb-worn device was used. Figure 1(a) shows the structure of smart-watch model for operation at 835, 1850, and 2450 MHz. The smart-watch model is a rectangular structure with 10 mm x 40 mm x 50 mm. The smart-watch model comprises a casing, display, battery, main board, and antenna part. The dielectric properties of the liquid-crystal-display (LCD) glass, LCD dielectric, and antenna carrier are based on those given by Ref. [6] and [7]. Figure. 1(b) shows return loss obtained by simulation based on this the smart-watch model.

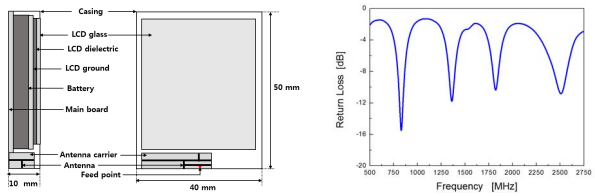

(a) (b)

Figure 1. (a) structure of smart-watch model and (b) its return loss

2.2 Calculation of SARs

The SAR distributions created by a smart-watch model in a flat phantom, two-body shape phantoms (wrist phantom and Specific Anthropomorphic Mannequin (SAM)), and anatomical human-body model. The long radius and short radius of simple wrist phantom are designed to be 30 mm and 15 mm respectively, and it is filled with wrist tissue [8]. The dielectric parameters of the flat phantom and SAM consists of a head tissue simulating liquid [1].

The anatomical human-body model are taken from Information Technologies in Society (IT'IS): Duke (34-year-old-male) [9]. The dielectric parameters of the anatomical human-body model were taken the 4-cole-cole model, which is based on measurements developed by Gabriel [10].

Regulation stipulate that the SAR of limb-worn devise be assessed in the two position: on writ and next-to-mouth.

For the wrist position, the rear side the smart-watch is placed in the contact with the flat phantom, wrist phantom, and anatomical wrist model, and the center of the wrist phantom and wrist model coincident with the centerline of the smart-watch (Figure 2).

For the next-to-mouth position, the smart watch is placed 10 mm from the flat phantom or 10 mm front of SAM and the anatomical head model (Figure 3).

For the wrist position, it is not necessary to consider the effect of the wrist. However, the user's wrist is included for obtaining conservative SAR estimations when the next to month. To begin, a simplified flat phantom and SAR model and wrist phantom were comparison with the more detailed model (Figure 4(a) and (b)). Next, realistic human wrist model was used (Figure 4(c) and (d)).

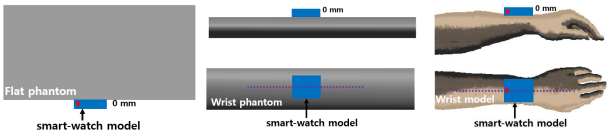

(a) Flat phantom (b) wrist phantom (c) human -wirst model.

Figure 2. Position of wrist-worn samrt-watch model for SAR caluction for flat phanom, wrist phantom, and antomical human wirst model.

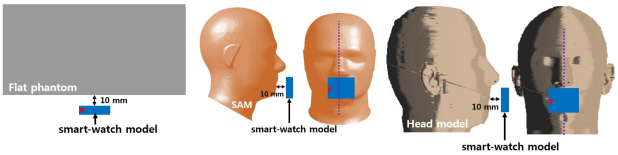

(a) Flat phantom (b) SAM model (c) human -head model.

Figure 3. Next-to-mouth position smart-watch model for SAR calculation for flat phantom, SAM and human-head models.

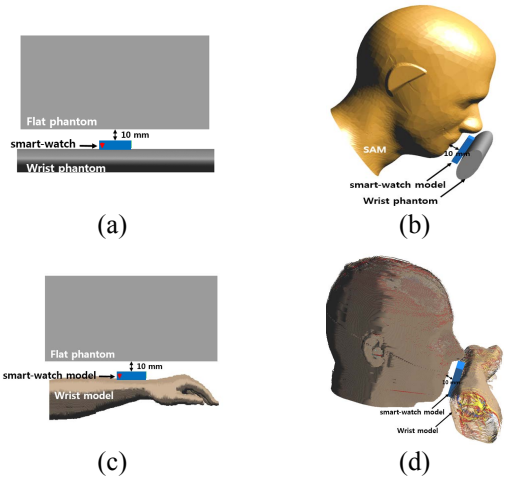

Figure 4. Next-to-mouth position : (a) flat phantom and wrist phantom (b) SAM phatnom and wrist phantom (c) flat phantom and human wrist model (d) head model and huamn wrist model

SAR distributions for the wrist watch model were calculated using the commercial electromagnetic simulation software SEMCAD X. All results in this paper are normalized to 1 W input power

3. Results

3.1 Calculation of SARs for wrist-worn smart-watch

The spatial peak 10-g SARs calculated from the flat phantom, the wrist phantom and human wrist models (Figure 5).

The calculated SARs are discussed as function of frequency in the smart-watch model. As shown in Figure 5, the flat phantom provides a conservative estimation of SAR for the wrist position at 835 MHz. However, at 1850 MHz and 2450 MHz, the smart-watch model produces higher SAR in the human-wrist model and wrist phantom than flat phantom.

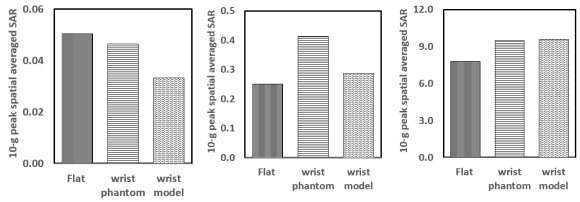

Figure 5. Spatial peak 10-g SARs of flat phantom, wrist phantm, and human wrist model at a frequency of (a) 835 MHz, (b) 1850 MHz (c) 2450 MHz.

3.2 Calculation of SARs for next-to-mouth smart-watch

Figure 6 shows the spatial peak 1- and 10-g SARs in flat phantom, SAM, and anatomical head model. As shown in Figure 5, the flat phantom provides a conservative estimation of SAR for the wrist position at 835 MHz. However, at 1850 MHz and 2450 MHz, the smart-watch model produces higher SAR in the human-wrist model and wrist phantom than flat phantom.

The spatial peak 1-and 10-g SARs in flat phantom and SAM model with and without wrist phantom are shown in Figure 7. The peak average SAR in the flat phantom and human head model are decreased when the wrist phantom is added to the flat phantom and human head model at 835. However, at 1850 MHz and 2450 MHz, The peak average SAR in flat phantom and head model with wirst model is lower than in the those without wirst mdoel.

Figure 8 show the spatial peak 1-and 10-g SARs in flat phantom and human head model with and without human wrist model. The peak average SAR in the flat phantom and human head model are increased when the wrist model is added to the flat phantom and human head model at 835. However, at 1850 MHz and 2450 MHz, The peak average SAR in flat phantom and head model without wirst model is higher in the those with wirst mdoel.

Figure 7 and Figure 8 results can be explained pargly by relfection at wrist phantom and wrist model boundary. In addtion, because of the spatial distribution of SAR depend on the interaction of reflected waves and the current distribution on the smart-watch model, the shape of the wrist model significantly impacts these results.

4. Conclusion

We report the results of SAR estimation for a smart watch with a monopole antenna at various frequencies. The SARs delivered by smart-watch were determined for flat phantom, homgenous body shape model, and antomical

human-body model, where the smart-wtach was either worn on the wirst or positioned next to the mouth. These results demonstrate that compliance testing for SAR using the flat phantom does not always yield a conservative.
A multi-varaiable investigation of the effect of the user's wirst in the terms of SAR in the flat phantom, SAM, and antomical head model has been conducted. It is found that the SAR cand be increaed significantly by presence of the wirsit for lower frequency.

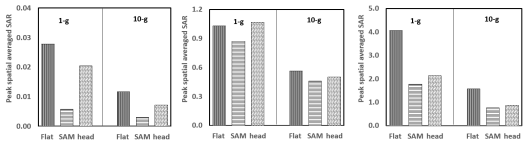

(a) (b) (c)

Figure 6. Spatial peak 1- and 10-g SARs of flat phantom, SAM model, and human head model at a frequency of (a) 835 MHz, (b) 1850 MHz (c) 2450 MHz.

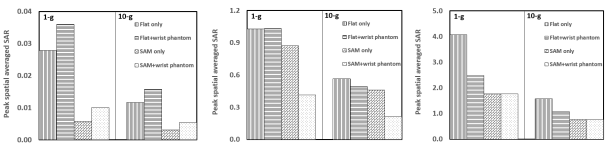

(a) (b) (c)

Figure 7. Spatial peak 1- and 10-g SARs of flat phantom, SAM model with and without wrist phantom at a frequency of (a) 835 MHz, (b) 1850 MHz (c) 2450 MHz.

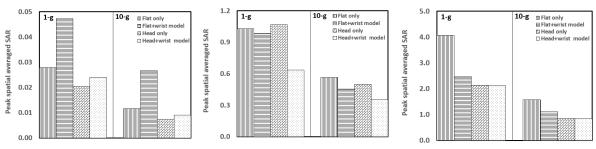

(a) (b) (c)

Figure 8. Spatial peak 1- and 10-g SARs of flat phantom, human head model with and without human wrist model at a frequency of (a) 835 MHz, (b) 1850 MHz (c) 2450 MHz.

Acknowledgements

This work was supported by the IT R&D program of MSIP/IITP/ [B0135-16-1002, Study on the EMF exposure control in smart society].

References

1. IEC 62209-2, 2010 Human exposure to radio frequency fields from hand-held and body mounted wireless communication devices – human models, instrumentation, and procedures – Part 2: Procedure to determine the specific absorption rate (SAR) for wireless communications devices used in close proximity to the human body (frequency range of 30 MHz to 6 GHz).
2. KDB 447498 D01 General RF Exposure Guidance v05r01 "Mobile and Portable Device RF Exposure Procedures and Equipment Authorization Policies," Office of Engineering and Technology Laboratory Division, Federal Communication Commission, May. 2013
3. C. H. Wu, K. L. Wong, and S. W. Su, "Internal shorted monopole antenna for the watch-type wireless communication device for Bluetooth operation," Microwave Optical Technology Letter, vol. 49, pp. 942–946, Apr. 2007.
4. C. H. Wu, K. L. Wong, Y.C. Lin, and S. W. Su, "Conformal Bluetooth Antenna for the Watch-Type Wireless Communication Device Application," IEEE Antennas and Propagation Society International Symposium, pp.4156 - 4159, 2007.
5. Kun Zhau et al., "Antenna designs of smart watch for cellular communications by using metal belt," European conference on Antennas and Propagation (EuCAP), pp. 1-5, 2015.
6. IEC/IEEE 62704-3(CD), Methods for the assessment of electric, magnetic and electromagnetic fields associated with human exposure.
7. N. Chavannes, R. Tay, N. Nikoloski, and N. Kuster, "Suitability of FDTD based TCAD tools for RF design of mobile phones," IEEE Trans. Antennas Propag., vol. 45, pp. 52–66, 2003.
8. CTIA "CTIA certification test plan for Device over-the air performance," 2016.
9. A. Christ et al., "The virtual family-development of surface-based anatomical models of two adults and two children for dosimetric simulations", Phys. Med. Biol., pp. N23-N38, 2010.
10. C. Gabriel, "Compilation of the dielectric poperties of body tissues at RF and microwwave frequencies," Occupational and environmental health directorate, Radiofrequency Radiation Division, Brooks Air Force Base, TX, Tech. Rep. N.AL/OE-TR-1996-0037, Jun. 1996.